https://doi.org/10.31891/2307-5732-2026-365-86
УДК 620.1.05

PROTSENKO VLADYSLAV
Kherson National Technical University
https://orcid.org/0000-0002-3468-4952
email: 1904pvo@gmail.com
RUSANOV SERGIY
Kherson National Technical University
https://orcid.org/0000-0002-1003-4867
email: serg.a.rusanov@gmail.com
KASYAN OLEKSIY
Kherson National Technical University
https://orcid.org/0009-0008-2039-6096
email: kasyan.aleksey@ukr.net

PRACTICE OF IMPROVING A SPRING TESTING MACHINE

The article deals with the practical issues of modernizing the machine for testing springs MIP 100-2 in order to be able to perform laboratory research. Using the methods of the theory of mechanisms and machines, in particular the contour method, the design of equipment for testing three- and four-point bending is substantiated, thereby eliminating extraneous loading of the samples through redundant connections. For the loader carriage drive motor, it is planned to use power from a single-phase network via a frequency converter, enabling smooth adjustment of the carriage speed over a range of up to 9. To eliminate the influence of the weight of the device on the value of the measured force, a plate-type strain gauge is installed on the moving carriage of the machine. The output of the strain gauge signal to its load indicators is carried out by using an amplification unit, indication and transmission of indicators, which can be displayed on its display and via a converter to a PC. The described measures have been tested in practice and have shown a positive result. An electrical circuit has been developed that can also provide the movement of the carriage in manual and automatic modes using limit switches, which allows you to reduce the time spent on performing multi-series tests and creates reserves for the development of automation of the testing process through the use of special loading and feeding devices. The proposed technical solutions are quite simple and accessible for practical implementation by means of repair shops. Provided that simple retrofitting is performed on the machine, it is possible to perform compression, shear, and other tests. UMM-5 and similar tensile machines can be improved using a similar strategy

Keywords: *testing machine, bending, compression, equipment, strain gauge, circuit method, redundant constraint.*

ПРОЦЕНКО ВЛАДИСЛАВ, РУСАНОВ СЕРГІЙ, КАСЯН ОЛЕКСІЙ
Херсонський національний технічний університет

ПРАКТИКА УДОСКОНАЛЕННЯ МАШИНИ ДЛЯ ВИПРОБУВАННЯ ПРУЖИН

Стаття присвячена практичним питанням модернізації машини для випробування пружин МИП 100-2 з метою можливості виконання лабораторних досліджень. Із використанням методів теорії механізмів і машин, зокрема поконтурного методу, обгрунтовано конструкцію оснащення для випробування на три- та чотириточковий згин, що виключає позаштатне навантаження зразків за рахунок виключення надлишкових зв'язків. Для двигуна приводу руху каретки навантажувача передбачено використати живлення від однофазної мережі через перетворювач частоти, що дає можливість забезпечення плавного регулювання швидкости руху каретки із діапазоном до 9. Для виколючення впливу ваги пристосування на величину вимірюваного зусилля на рухомій каретці машини встановлено тензометричний силовимірювач тарілчастого типу. Ввиведення сигналу тензодавача на показники його навантаження виконано за рахунок використання блока підсилення, індикації та передавання показників, які можуть виводитись на його табло та через перетворювач на ПК. Описані заходи апробовані на практиці і показали позитивний результат. Розроблена електрична схема, що може забезпечити також рух каретки нв ручному та автоматичному режимі по кінцевих вимикачах, що дозволяє скоротити витрати часу при виконанні багатосерійних випробувань та створює резерви для розвитку автоматизації процесу випробування за рахунок застосування спеціальних завантажувально-подавальних пристроїв. Запропоновані технічні рішення достатньо прості і доступні до реалізації на практиці засобами ремонтних майстерень. За умови виконання нескладного дооснащення на машині можливо виконувати випробування на стискання, зріз та інші. За подібною стратегією можуть бути удосконалені розривні машини УММ-5 і подібні.

Ключові слова: *випробувальна машина, згин, стискання, оснащення, тензодавач, поконтурний метод, надлишковий зв'язок.*

Стаття надійшла до редакції / Received 17.03.2026
Прийнята до друку / Accepted 14.04.2026
Опубліковано / Published 28.05.2026

This is an Open Access article distributed under the terms of the Creative Commons CC-BY 4.0

© Проценко Владислав, Русанов Сергій, Касян Олексій

Introduction

The development of new materials and products manufactured from them requires precise knowledge of their properties, as well as the influence of processing technologies and operating conditions, which ultimately determine production cost [1]. Of particular importance is the study of plastic materials, which enable the implementation of resource-saving approaches and thereby reduce the cost of finished products.

Literature review

In study [2], the mechanical behavior of Acrylonitrile-Butadiene-Styrene (ABS), one of the most important amorphous thermoplastics, was investigated to determine the influence of testing conditions on the elastic properties of the material. ABS is widely used due to its high impact toughness, strength, and thermal resistance; however, its flexural behavior-especially under varying loading conditions-required detailed examination to predict failure zones and energy absorption characteristics. The authors conducted a series of four-point bending tests at different deformation rates and

two support span lengths to evaluate their influence on mechanical parameters. Comparative data were also obtained through numerical modeling. The experiments made it possible to measure reaction forces versus deflection, assess flexural strength, and characterize the material's behavior under bending loads. It was established that the elastic properties of ABS significantly depend on span length and loading rate. For shorter spans, the post-peak force decreased more abruptly, indicating more severe internal damage accumulation under such conditions.

Article [3] focuses on the effect of strain rate on the elastic properties of a material reinforced with continuous carbon fibers in a polyamide 6 matrix (CF-PA6). This plastic is gaining popularity in lightweight structures where a combination of high strength and low weight is critical, for example, in automotive applications. Under near-service conditions, materials may experience loads applied at different rates; therefore, understanding rate-dependent behavior is essential. Four-point bending tests were performed at three strain rates: quasi-static, intermediate, and high. The results demonstrated that the flexural strength of CF-PA6 does not exhibit a clear dependence on strain rate within the investigated range. Similarly, the strain at failure (~1.05–1.10%) and the elastic modulus (~101–102 GPa) showed no significant variation. Using digital image correlation and high-speed video recording, the authors traced the failure mechanism. Regardless of loading rate, failure initiated with compressive fiber fracture and delamination of outer layers, followed by crack propagation into the tensile zone. Statistical analysis showed that the strength distribution follows a two-parameter Weibull model without a pronounced dependence on loading rate.

In study [4], the authors examined the influence of aggressive environments on the elastic properties of polyoxymethylene, an important thermoplastic widely used in bearings, gears, and mechanical components, where the material may be exposed to liquids or ultraviolet radiation. Ten samples were exposed to five different environments: ambient atmosphere, distilled water, lubricating oil, ultraviolet radiation, and saline solution. After prolonged exposure, four-point bending tests were performed to determine the maximum flexural stress. The results indicated that exposure to distilled water, cooling oil, and saline solution led to a reduction in maximum bending force, demonstrating material degradation in these environments. Ultraviolet radiation caused an increase in flexural stress, suggesting increased stiffness due to UV-induced structural changes.

Article [5] investigated the influence of Fused Deposition Modeling (FDM) process parameters on the elastic properties of samples made from polyethylene terephthalate glycol (PETG) and recycled PETG (rPETG). The main objective was to determine which printing parameters affect maximum flexural strength and whether recycled material can be used in engineering practice without significant loss of mechanical properties, which is important for recycling and zero-waste manufacturing concepts. Samples were subjected to three-point bending tests using a universal testing machine to determine maximum flexural stress under standard testing conditions. Regression analysis was applied to evaluate the statistical significance of printing parameters. Based on the experiments, it was concluded that rPETG used in the FDM process exhibits competitive mechanical properties, particularly at high infill densities, highlighting the feasibility of using recycled materials for part production. This not only reduces manufacturing costs but also reduces environmental impact by utilizing plastic waste.

Study [6] is devoted to the development and implementation of an automated system for conducting three-point bending tests of PLA/TPU polymer blends with TPU content ranging from 0% to 100%. The primary objective was to ensure high-throughput automated testing to obtain large datasets on mechanical and physical properties with minimal human intervention, which is particularly relevant for modern research on composite and hybrid polymers. The study involved the creation of a robotic setup consisting of a robotic manipulator, a sample storage table, and a testing machine. The system enabled continuous sample feeding into the testing machine and automated three-point bending tests of standardized samples in accordance with ISO 20753:2019-01. A total of 628 PLA/TPU samples with varying TPU content (0%, 10%, 25%, 40%, 70%, 90%, 100% by weight) were tested. It was shown that flexural strength and modulus of elasticity decrease monotonically with increasing TPU content. This is explained by the transition from rigid thermoplastic PLA to more elastic TPU, which reduces the material's ability to sustain high bending loads. The processed results demonstrated high coefficients of determination ($R^2 \approx 1$) for regression curves, indicating a strong correlation between TPU concentration and flexural characteristics. Thus, the study demonstrates the high efficiency of the robotic testing system, enabling rapid data acquisition and high-precision results.

Therefore, a review of current research shows that the determination of elastic modulus and ultimate flexural stress of plastic samples is typically performed using three- or four-point bending schemes with the sample supported on spans [7–9].

The implementation of modern laboratory research in mechanics and materials science using outdated testing machines and equipment commonly available in Ukrainian laboratories has significant drawbacks. These are primarily related to the remoteness of the force-measuring element (usually a spring) from the loading device within the force-measuring chain, which introduces measurement errors due to the lever system's friction and joint clearances. Another disadvantage is the obsolescence of the electrical system, including power supply from a three-phase network in some cases via a bulky external unit, and the lack of smooth speed control of the loading carriage.

The analysis of practical case studies has shown that modernization of such equipment is carried out in several directions. The first involves retaining the standard force-measuring chain while installing a resistive sensor to measure the angular displacement of the force-indicating pointer [10], or recording acoustic emission signals [11], without upgrading the loading drive. This allows data transmission to a personal computer (PC), but it does not eliminate the effects of clearances and friction in the lever joints, nor does it provide smooth speed control of the loading device. The second, more advanced approach involves the use of strain gauges positioned directly near the tested sample, with data transmission to a PC [12], again without modernizing the loading drive. This eliminates the adverse effect of the lever-based force-measuring

system but still does not enable smooth speed regulation. An even more advanced third option [13] includes the use of strain gauge force sensors located directly near the sample, combined with a stepper motor driving the loading mechanism.

Problem statement

In the latter configuration, where a stepper motor enables smooth speed control, several disadvantages remain. Such modernization requires modifying the motor-to-transmission connection, fabricating an adapter plate, and, if necessary, a coupling. Another drawback is the possibility of non-standard (misaligned or unintended) loading of the tested sample when using the implemented fixture.

This can be demonstrated using the example of four-point bending tests of plastic samples to determine ultimate flexural stress or elastic modulus. The mechanism of the MIP-100 testing machine applied in [13] includes carriage 1 (Fig. 1), which moves via a chain drive along the prismatic guides of its frame 0. Mounted on carriage 1 is the upper plate 2, to which an adapter plate 3 is attached. On spacer 4, the upper pair of rollers 5 is installed; these apply load to the sample 6. The sample rests on the lower pair of rollers 7, which are mounted on spacers 8 fixed to the lower plate 9. The lower plate 9 is installed on the lower platen 10, which transmits the force to the force-measuring mechanism.

Sample 6 must be loaded by forces applied along the axis of symmetry of its cross-section through the cylindrical rollers 5 and 7. To ensure correct loading conditions, these rollers must provide linear contact with the sample (Fig. 2a).

The described mechanism contains $n = 6$ movable links (carriage 1 with parts fixed to it, two pairs of rollers 5 and 7, sample 6). The number of fifth class kinematic pairs here $P_5 = 5$ (A_5, B_5, C_5, M_5, N_5), number of second class kinematic pairs $P_2 = 4$ (R_2, S_2, Q_2, T_2), other class pairs are absent $P_4 = P_3 = P_1 = 0$.

The total kinematic pairs number is:

$$P = P_5 + P_4 + P_3 + P_2 + P_1 = 5 + 0 + 0 + 4 + 0 = 9. \quad (1)$$

The sum of the kinematic pairs movabilities:

$$f = 1P_5 + 2P_4 + 3P_3 + 4P_2 + 5P_1 = 1\times5 + 2\times0 + 3\times0 + 4\times4 + 5\times0 = 21. \quad (2)$$

Number of independent locked circuits by Gohman formula:

$$k = P - n = 9 - 6 = 3. \quad (3)$$

Independent locked circuits are: $M_5Q_2T_2N_5M_5$; $B_5R_2S_2C_5B_5$; $N_5T_2S_2C_5A_5N_5$.

Total mechanism mobility by Voinea and Atanasiu equation:

$$W = f - \sum r_i = 21 - (5 + 5 + 4) = 7, \quad (4)$$

where r_i – independent locked circuit axes rank.

$$W = W_b + W_l = 0 + 7 = 7, \quad (5)$$

where $W_b = 0$ – mechanism basic mobility;

$W_l = 7$ – links local mobilities (rollers 5, 7 around Z axis (4 mobilities), sample 6 along X and Z axes, and also around Y axis (3 mobilities)).

Then the redundant constraints number in the basic variant by Somov and Malyshev formula:

$$q_{SM} = W + 5P_5 + 4P_4 + 3P_3 + 2P_2 + P_1 - 6n = \\ = 7 + 5\times5 + 4\times0 + 3\times0 + 2\times4 + 0 - 6\times6 = 4. \quad (6)$$

Redundant constraints number by Ozols formula:

$$q_{OZ} = W + 6k - f = 7 + 6\times3 - 21 = 4. \quad (7)$$

Using the circuit method of L.N. Reshetov confirms the presented calculations (table 1) [14, 15] (table. 1), it allows to set redundant constraints location.

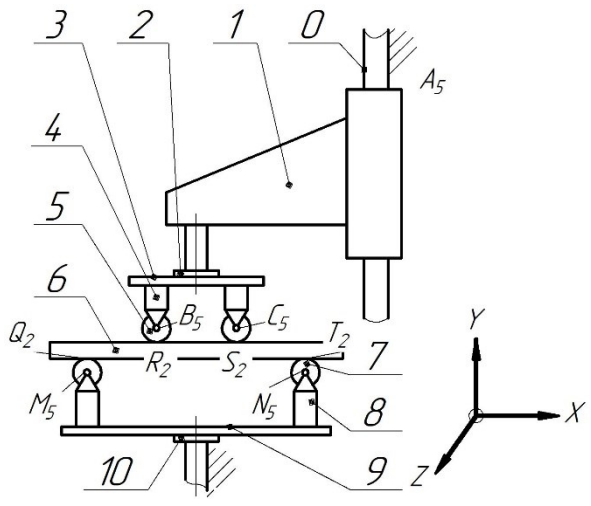

Fig. 1. General view of the mechanisms and equipment of the MIP-100 machine during the four-point bending test in the basic version

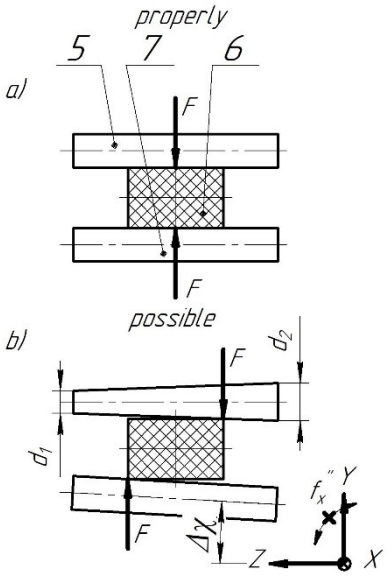

Fig. 2. Properly (a) and possible (b) options for applying load to the sample

Redundant constraints q_1 and q_2 do not usually affect the load on the specimen, as gaps in the kinematic pair A along the X and Z axes usually level them. Redundant constraints q_3 and q_4 can lead to point contact of the rollers with the sample at the edges of the cross-section (Fig. 2, b) instead of the center, as it should be. This can occur, for example, with manufacturing errors of spacers 4 and 8 (Fig. 1) in height, angular deviation $\Delta\chi$ of the roller axes from the Z axis in the ZY plane, non-alignment of the roller axes of each pair to the same plane, roller taper ($d_1 \neq d_2$), non-planarity of the supporting surface of the sample, or a combination of these factors. As a result, the sample can undergo torsion deformation and unforeseen contact loads.

Table 1.

Circuit method application of to the loading mechanism of a prismatic sample in four-point bending in the basic version

Circuit	Planar movabilities f_p	Non-planar movabilities f_n
$M_5Q_2T_2N_5M_5$	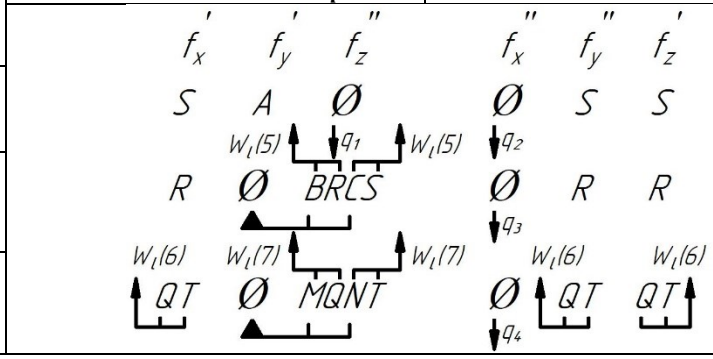	
$B_5R_2S_2C_5B_5$		
$N_5T_2S_2C_5A_5N_5$		
$W = 7,\ q = 4$		

Aims of the article

The main task of the article is to improve the MIP-100-2 testing machine available in the laboratory of the Kherson National Technical University to ensure:

- reducing the number of redundant constraints in the equipment of testing samples for bending according to four-point and three-point schemes, and thereby eliminating the possibility of abnormal loading of the tested samples;
- improving the loader drive to ensure the possibility of power supply from a single-phase network, smooth start-up, and adjustment of the carriage speed in manual or automatic mode;
- excluding the lever system from the force measuring circuit in order to increase the accuracy of determination and avoid the influence of the weight of the device on the value of the measured force;
- achieving the connection of the machine with a PC for the purpose of data transfer and remote control.

Methods

To improve the structural efficiency of the machine equipment by determining the locations and eliminating redundant constraints, methods of the Theory of Mechanisms and Machines were applied, in particular, the L. Reshetov circuit method, as well as the methods of Ozols and Voinia-Atanasiu. The calculations were performed using the Maxima computer algebra system, graphical constructions were created in SolidWorks, Paint, graphs built in MS Excel, the search for information on samples bending tests in modern researches and using equipment was conducted using ChatGPT-5.

Main material presentation

To achieve the first point, equipment was developed for testing plastic samples in four- and three-point bending. Next, we will estimate the number of redundant constraints when using the proposed equipment for testing in four- and three-point schemes.

The MIP-100-2 machine is somewhat different from the MIP-100 machine, it contains a carriage 1 (Fig. 3), which moves vertically along vertical cylindrical guides fixed to the frame 0. A plate 2 with a strain gauge is rigidly fixed to the carriage 1. When testing in a four-point scheme, it is proposed to attach a traverse 3 to the strain gauge with a rotating hinge, where the upper pair of rollers 5 is fixed in the rotary housings 4, which press on the sample 6. The sample 6 is placed on the lower pair of rollers 7, which are rigidly mounted on the frame of the machine 0; one of these rollers is mounted on a hinged support 8.

The described mechanism contains $n = 10$ movable links (carriage 1 with parts fixed to it, traverse 3, housings 4, two pairs of rollers 5 and 7, sample 6, hinged support 8). The number of fifth class kinematic pairs here $P_5 = 5$ (I_5, J_5, E_5, K_5, M_5, N_5, O_5, U_5), number of fourth class kinematic pairs $P_4 = 2$ (A_4, B_4), number of second class kinematic pairs $P_2 = 4$ (R_2, S_2, Q_2, T_2), other class pairs are absent $P_3 = P_1 = 0$.

The total kinematic pairs number is:

$$P = P_5 + P_4 + P_3 + P_2 + P_1 = 8 + 2 + 0 + 4 + 0 = 14.$$

The sum of kinematic pairs movabilities:

$$f = 1P_5 + 2P_4 + 3P_3 + 4P_2 + 5P_1 = 1\times8 + 2\times2 + 3\times0 + 4\times4 + 5\times0 = 28.$$

Number of independent locked circuits by Gohman formula:

$$k = P - n = 14 - 10 = 4.$$

Independent locked circuits are: $A_4O_5I_5M_5R_2T_2E_5U_5A_4$; $B_4O_5J_5N_5S_2Q_2K_5B_4$; $M_5I_5J_5N_5S_2R_2M_5$; $U_5E_5T_2Q_2K_5U_5$.

Total mechanism mobility by Voinea and Atanasiu equation:

$$W = f - \sum r_i = 21 - (5 + 5 + 4) = 7.$$

$$W = W_b + W_l = 0 + 7 = 7,$$

where $W_b = 0$ – mechanism basic mobility;

$W_l = 7$ – links local mobilities (rollers 5, 7 around Z axis (4 mobilities), sample 6 along X and Z axes, and also around Y axis (3 mobilities)).

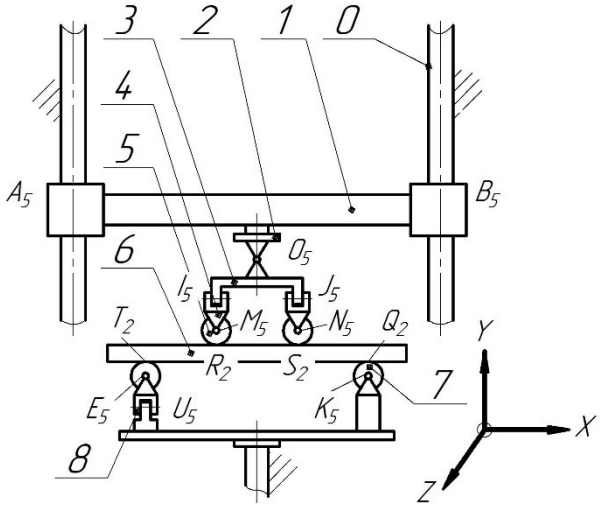

Fig. 3. General view of the mechanisms and equipment of the MIP-100-2 machine during the four-point bending test in the improved version

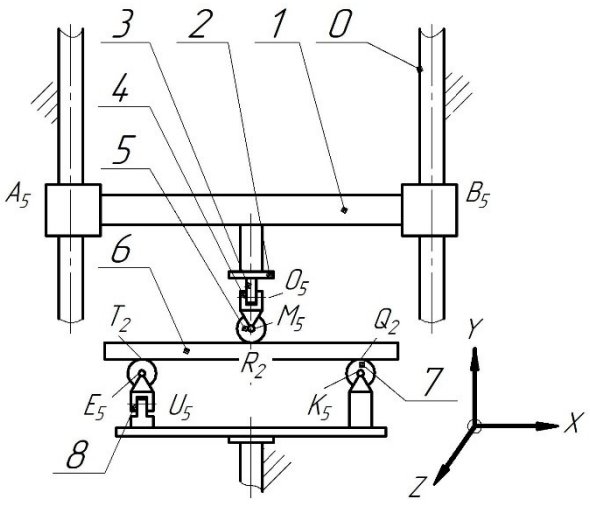

Fig. 4. General view of the mechanisms and equipment of the MIP-100-2 machine during the three-point bending test in the improved version

Redundant constraints number in the basic variant by Somov and Malyshev formula:

$$q_{SM} = W + 5P_5 + 4P_4 + 3P_3 + 2P_2 + P_1 - 6n = 7 + 5 \times 8 + 4 \times 2 + 3 \times 0 + 2 \times 4 + 0 - 6 \times 10 = 3.$$

Redundant constraints number by Ozols formula:

$$q_{OZ} = W + 6k - f = 7 + 6 \times 4 - 28 = 3.$$

The presented calculations confirm the use of the circuit method (Table 2), where it is seen that there are no redundant constraints directly in the contours formed by the kinematic pairs of equipment that provide the load on the sample.

Table 2.

Circuit method application to the loading mechanism of a prismatic sample in four-point bending in the improved version

Circuit	Planar movabilities f_p	Non-planar movabilities f_n
$A_4O_5I_5M_5R_2T_2E_5U_5A_4$	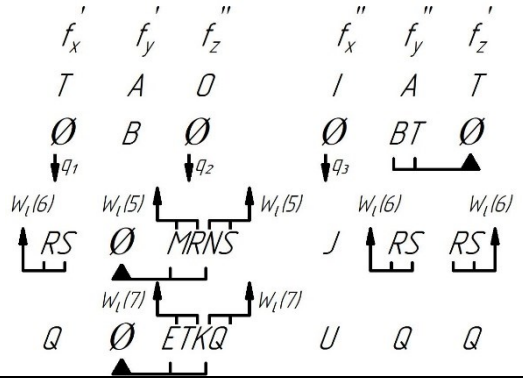	
$B_4O_5J_5N_5S_2Q_2K_5B_4$		
$M_5I_5J_5N_5S_2R_2M_5$		
$U_5E_5T_2Q_2K_5U_5$		
$W = 7,\ q = 3$		

When testing for three-point bending, we will have a scheme according to Fig. 4. Here, on carriage 1, in the strain gauge fixed on the upper plate 2, a holder 3 is installed, on which the support 4 of the upper roller 5 is hingedly mounted. The roller 5 presses on the sample 6, which is mounted on the lower pair of rollers 7, which are rigidly mounted on the machine frame 0; one of these pair of rollers is mounted on a hinged support 8.

Described mechanism contains $n = 7$ movable links (carriage 1 with parts fixed to it, hinged support 4, rollers 5 and 7, sample 6, hinged support 8). The number of fifth class kinematic pairs here $P_5 = 5$ (E_5, K_5, M_5, O_5, U_5), number of fourth class kinematic pairs $P_4 = 2$ (A_4, B_4), number of second class kinematic pairs $P_2 = 3$ (R_2, Q_2, T_2), other class pairs are absent $P_3 = P_1 = 0$.

The total kinematic pairs number is:

$$P = P_5 + P_4 + P_3 + P_2 + P_1 = 5 + 2 + 0 + 3 + 0 = 10.$$

The sum of kinematic pairs movabilities:

$$f = 1P_5 + 2P_4 + 3P_3 + 4P_2 + 5P_1 = 1\times5 + 2\times2 + 3\times0 + 4\times3 + 5\times0 = 21.$$

Number of independent locked circuits by Gohman formula:

$$k = P - n = 10 - 7 = 3.$$

Independent locked circuits are: $A_4O_5M_5R_2T_2E_5U_5A_4$; $B_4O_5M_5R_2Q_2K_5B_4$; $U_5E_5T_2Q_2K_5U_5$.

Total mechanism mobility by Voinea and Atanasiu equation:

$$W = f - \sum r_i = 21 - (5 + 5 + 5) = 6.$$

$$W = W_b + W_l = 0 + 6 = 6,$$

where $W_b = 0$ – mechanism basic mobility;

$W_l = 6$ – links local mobilities (rollers 5, 7 around Z axis (3 mobilities), sample 6 along X and Z axes, and also around Y axis (3 mobilities)).

Redundant constraints number in basic variant by Somov and Malyshev formula:

$$q_{SM} = W + 5P_5 + 4P_4 + 3P_3 + 2P_2 + P_1 - 6n = 6 + 5\times5 + 4\times2 + 3\times0 + 2\times3 + 0 - 6\times7 = 3$$

Redundant constraints number by Ozols formula:

$$q_{OZ} = W + 6k - f = 6 + 6\times3 - 21 = 3.$$

The presented calculations confirm the use of the circuit method (Table 3), where it is seen that there are no redundant constraints directly in the contours formed by the kinematic pairs of equipment that provide the load on the sample.

Table 3.

Circuit method application to the loading mechanism of a prismatic sample in three-point bending in the improved version

Circuit	Planar movabilities f_p	Non-planar movabilities f_n
$A_4O_5M_5R_2T_2E_5U_5A_4$	f_x' f_y' f_z'' T A O Ø B Ø q_1 $W_l(7)$ q_2 $W_l(7)$ Q Ø ETKQ	f_x'' f_y'' f_z' M A T Ø BT Ø q_3 U Q Q
$B_4O_5M_5R_2Q_2K_5B_4$		
$U_5E_5T_2Q_2K_5U_5$		
$W = 6,\ q = 3$		

To ensure the possibility of power supply from a single-phase network, soft start and adjustment of the carriage speed in manual or automatic mode, the machine loader drive was generally left unchanged, but a VFC-M0701S frequency converter was used (Fig. 5, Table 4), which provides power to the basic three-phase electric motor from a single-phase 230 V network. The basic AOL 12/4 motor was reconnected from a “delta” to a “star” connection and equipped with fuses (3.0 A at a nominal current of 0.6 A) for each phase.

Fig. 5. Frequency converter general view

Fig. 6. Load cell general view

Fig. 7. Indication unit general view

The change in current frequency with such an improvement can be performed smoothly manually or controlled from a PC via the RS485 interface. In this case, the speed V (mm/min) of the machine loading carriage movement with changes in current frequency is calculated by the formula (Fig. 8):

$$V = \frac{f}{p}\left[1 - \frac{s}{100\%}\right]\frac{z_s}{z_w} z_{sc} t_{sc}, \quad (8)$$

where f – motor supply current frequency, Hz; $p = 2$ – number of pairs of poles of the electric motor winding;

s = 6,7 % – slip; z_s – number of steps of the worm gear reducer; $z_к$ – number of teeth of the worm wheel (z_s / z_w = 1/12); z_{sc} = 2 – number of steps of the lead screw; t_{sc} = 5 mm – lead screw thread pitch.

Table 4.

Technical characteristics of the frequency converter VFC-M0701S

Model	VFC-M0701S
Maximum operating power	1,5 kW
Supply voltage	200 - 240 V AC, 50/60 Hz
Range of possible output frequency change	1 - 99 Hz
Pulse width modulation reference frequency	8 kHz
Maximum output current	3,86 A
Own consumption	<20 W
Built-in active cooling system (fan)	+
Communication protocol	RS-485/Modbus
Built-in potentiometer	+
Dimensions	130×105×60 mm×mm×mm
Mass	335 g

To eliminate the influence of the weight of the device on the magnitude of the measured deformation force, a plate-type strain gauge is installed on the upper plate of the moving carriage of the loader (Fig. 6, Table 5). The output of the transformation of the change in the parameters of the strain gauge into its load indicators is performed by using the KV-4A RS485 amplification, indication, and transmission unit (Fig. 7, Table 6) on its display and through the converter to the PC. The verification of the devices installed in the force-measuring chain is planned to be performed with a sample dynamometer of the DOSM 3-0.2 type.

Table 5.

Technical characteristics of the LCF-2D load cell

Model	LCF-2D
Type of load	Compression and tension
Maximum load, F_{max}	200 kg
Measurement error, % F_{max}	±0,03
Zero return error, % F_{max}	±0,03
Minimum load, F_{min}	0
Maximum overload,% F_{max}	150
Maximum excitation voltage, U_{max}	10 - 15 B
Input resistance	750±20 Om
Output resistance	700±5 Om
Insulation resistance	≥5000 Om
Operating temperature range	-20…+80 °C
Housing material	Steel
Dimensions	88×34 mm×mm

Table 6.

Technical characteristics of the KV-4A RS485 amplification, indication, and transmission unit

Model	KV-4A RS485
Supply voltage	24 V DC or 220 V AC
Load Capacity	Supports up to 8 × 350Ω sensors
Own consumption	5 W
Sampling frequency	1000 Hz
Housing material	Plastic
Communication protocol	RS-485/Modbus
Operating temperature range	-25-+45°C
Dimensions	96×48×110 mm×mm×mm
Mass	0,3 kg

The connection of the frequency converter, strain gauge, and carriage displacement sensor with a PC is possible via the RS485 interface, which allows for automated reading and recording of the indicators taken during testing, as well as loading of samples subjected to testing according to a predetermined program.

To install the new machine equipment, a steel adapter washer was made on the upper plate for installing the strain gauge, and a new adapter panel was also made using 3D printing (Fig. 9). The result of the change in spring force over time, obtained during its testing, is shown in Fig. 10.

If high repeatability of experiments is required, the electrical circuit of the loader drive can be improved according to Fig. 11, which provides the possibility of moving the loader carriage in manual or automatic mode using limit switches or programmed from a PC.

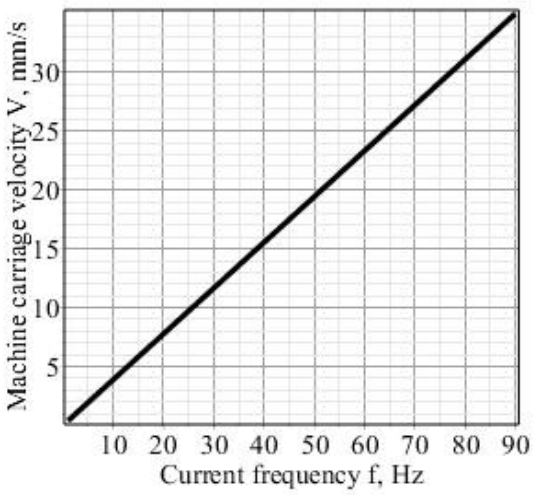

Fig. 8. Graph of the dependence of the carriage speed *V* on the current frequency *f* in the improved machine

Fig. 9. Photo of the improved MIP 100-2 machine

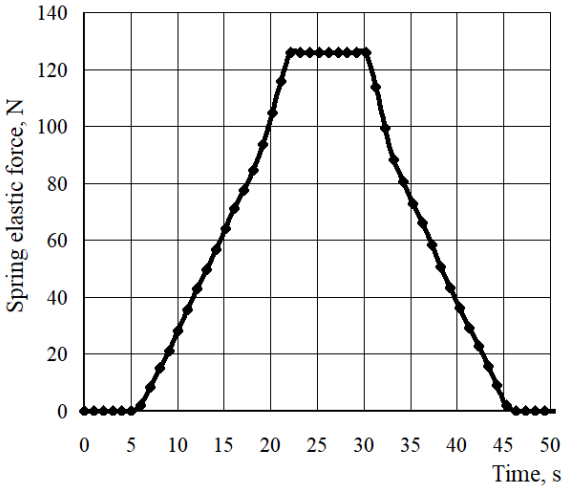

Fig. 10. Diagram of the change in spring elastic force over time

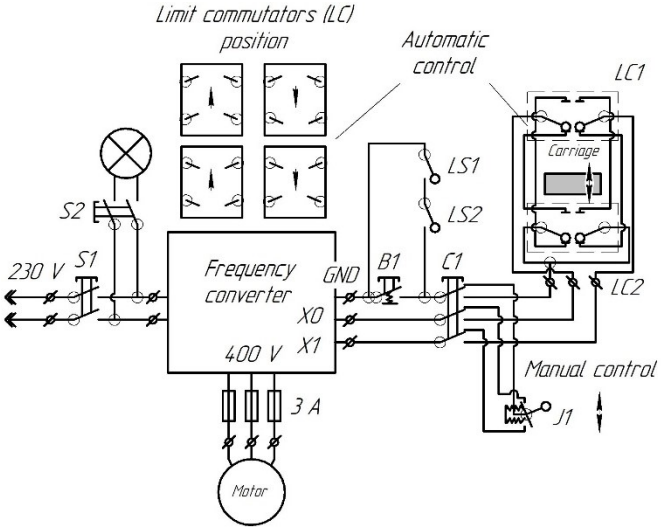

Fig. 11. Electrical diagram of the loader drive of the improved machine MIP 100-2

Conclusions

By analyzing the experience of modernization of Soviet-built testing machines in the laboratories of Ukrainian research institutions, an improvement of the MIP 100-2 spring testing machine was proposed and implemented. The design of the equipment for testing three- and four-point bending was substantiated, which eliminates the extraneous loading of samples. It is planned to power the drive of the loader carriage from a single-phase network through a frequency converter, which makes it possible to ensure smooth regulation of its speed with a range of up to 9. To eliminate the influence of the weight of the device on the value of the measured deformation force, a plate-type strain gauge was installed on the upper plate of the moving loader carriage. The output of the signal of the transformation of the strain

gauge parameters into its load indicators was performed by using an amplification, indication, and transmission unit, which can be displayed on its display and via a converter to a PC. The developed electrical circuit also provides for the movement of the loader carriage in manual and automatic modes using limit switches, which allows reducing the time spent on performing multi-series tests and creates reserves for the development of automation of the testing process through the use of special loading and unloading devices.

References

1. Protsenko, V. O., & Kasyan, A. O. (2025). Features of development and implementation of products from new composite materials // Scientific Bulletin of Kherson State Maritime Academy. – 2025. – № 1(30). – С. 118–131. – DOI: https://doi.org/10.33815/2313-4763.2025.1.30.118-131.
2. Dhaliwal G. S., Dundar M. A. Four point flexural response of acrylonitrile-butadiene–styrene // Journal of Composites Science. – 2020. – Vol. 4, № 2. – Art. 63. – DOI: https://doi.org/10.3390/jcs4020063.
3. Jung J., Schmiedt M., Schneider R., Rimkus W., Taha I. Experimental investigation on the strain rate dependence of continuous carbon fibre reinforced PA6 under four point flexural loading // Applied Composite Materials. – 2026. – Vol. 33. – Art. 37. – DOI: https://doi.org/10.1007/s10443-025-10390-w.
4. Pascu A. M., Petrașcu O. L. Evaluating the flexural properties of polyoxymethylene under aggressive environmental conditions // Acta Universitatis Cibiniensis – Technical Series. – 2024. – Vol. 76. – DOI: https://doi.org/10.2478/aucts-2024-0005.
5. Iacob D. V., Zisopol D. G., Minescu M. Study on the optimization of FDM parameters for the manufacture of three-point bending samples from PETG and recycled PETG // Materials. – 2025. – Vol. 18. – Art. 4280. – DOI: https://doi.org/10.3390/ma18184280.
6. Robotization of three-point bending mechanical tests using PLA/TPU blends as an example in the 0–100% range // Materials. – 2023. – Vol. 16, № 21. – Art. 6927. – DOI: https://doi.org/10.3390/ma16216927.
7. ГОСТ 9550–81. Пластмаси. Метод визначення модуля пружності при згині. – Введ. 01.01.1982. – М.: Держстандарт СРСР, 1981. – 12 с.
8. ISO 178:2019. Plastics – Determination of flexural properties. – Geneva: International Organization for Standardization, 2019. – 32 p.
9. ASTM D790–23. Standard Test Methods for Flexural Properties of Unreinforced and Reinforced Plastics and Electrical Insulating Materials. – West Conshohocken: ASTM International, 2023. – 16 p.
10. Melnychenko, A. O., Rubanka, M. M., Misiats, V. P., & Polishchuk, O. S. (2020). Improvement of the UMM-5 machine for determining mechanical characteristics of structural materials // Herald of Khmelnytskyi National University. Technical Sciences. – 2020. – № 6(291). – С. 93–100. – DOI: https://doi.org/10.31891/2307-5732-2020-291-6-93-100.
11. Aleksenko V. L., Sharko A. A., Smetankin S. A., Stepanchykov D. M., Yurenin K. Y. Application of acoustic emission and strain gauge measurements to diagnostics of strain hardening processes in epoxy matrix composites // Technical Diagnostics and Non-Destructive Testing. – 2019. – № 3. – С. 46–54. – DOI: https://doi.org/10.15407/tdnk2019.03.07.
12. Podnebenna S. K., Burlaka V. V., Hulakov S. V., Kysliak V. H. Modernization of the 2167R-50 tensile testing machine for investigating the strength of welded joints // Bulletin of the Pryazovskyi State Technical University. Technical Sciences. – 2018. – № 36. – С. 113–119. – DOI: https://doi.org/10.31498/2225-6733.36.2018.142532.
13. Aleksenko V. L., Yurenin K. Y., Tatarintseva Y. H., Fostyk P. P., Vasylchenko H. Y., Znamerovska N. P., Onyshko D. M. Circuit design solutions in the renovation of testing equipment // Scientific Bulletin of Kherson State Maritime Academy. – 2024. – № 1(28). – С. 93–103. – DOI: https://doi.org/10.33815/2313-4763.2024.1.28.093-103.
14. Protsenko V., Malashchenko V., Babii M., Nastasenko V., Protasov R., Brumerčík F., Macko M. Redundant constraints in crane disc brake mechanism: Effect and disposal perspectives // Communications – Scientific Letters of the University of Žilina. – 2025. – Vol. 29. – DOI: https://doi.org/10.26552/com.C.2025.029.
15. Meneghini L., Noal Artmann V., Simoni R., Simas H. Mobility analysis and self-alignment of a novel asymmetric 3T parallel manipulator // Multibody Mechatronic Systems. MuSMe 2021. Mechanisms and Machine Science. – 2021. – Vol. 94. – P. 133–144. – DOI: https://doi.org/10.1007/978-3-030-60372-4_11.

Література

1. Проценко В. О., Касян А. О. Особливості розроблення та впровадження виробів з нових композитних матеріалів // Науковий вісник Херсонської державної морської академії. – 2025. – № 1(30). – С. 118–131. – DOI: https://doi.org/10.33815/2313-4763.2025.1.30.118-131.
2. Dhaliwal, G. S., & Dundar, M. A. (2020). Four point flexural response of acrylonitrile-butadiene–styrene. *Journal of Composites Science, 4*(2), 63. https://doi.org/10.3390/jcs4020063
3. Jung, J., Schmiedt, M., Schneider, R., Rimkus, W., & Taha, I. (2026). Experimental investigation on the strain rate dependence of continuous carbon fibre reinforced PA6 under four point flexural loading. *Applied Composite Materials, 33*, 37. DOI: https://doi.org/10.1007/s10443-025-10390-w
4. Pascu, A. M., & Petrașcu, O. L. (2024). Evaluating the flexural properties of polyoxymethylene under aggressive environmental conditions. *Acta Universitatis Cibiniensis – Technical Series, 76*. DOI: https://doi.org/10.2478/aucts-2024-0005
5. Iacob, D. V., Zisopol, D. G., & Minescu, M. (2025). Study on the optimization of FDM parameters for the manufacture of three-point bending samples from PETG and recycled PETG. *Materials, 18*, 4280. DOI: https://doi.org/10.3390/ma18184280

6. Robotization of three-point bending mechanical tests using PLA/TPU blends as an example in the 0–100% range. (2023). *Materials, 16*(21), 6927. DOI: https://doi.org/10.3390/ma16216927

7. ГОСТ 9550–81. Пластмаси. Методи визначення модуля пружності при згині. – Введ. 01.01.1982. – М.: Держстандарт СРСР, 1981. – 12 с.

8. International Organization for Standardization. (2019). *ISO 178:2019. Plastics - Determination of flexural properties.*

9. ASTM International. (2023). *ASTM D790-23: Standard test methods for flexural properties of unreinforced and reinforced plastics and electrical insulating materials.*

10. Мельниченко А. О., Рубанка М. М., Місяць В. П., Поліщук О. С. Удосконалення машини УММ-5 для визначення механічних характеристик конструкційних матеріалів // Вісник Хмельницького національного університету. Технічні науки. – 2020. – № 6(291). – С. 93–100. – DOI: https://doi.org/10.31891/2307-5732-2020-291-6-93-100.

11. Алексенко В. Л., Шарко А. А., Сметанкін С. А., Степанчиков Д. М., Юренін К. Ю. Application of acoustic emission and strain gauge measurements to processes of diagnostics of strain hardening of epoxy matrix composites // Technical Diagnostics and Non-Destructive Testing. – 2019. – № 3. – С. 46–54. – DOI: https://doi.org/10.15407/tdnk2019.03.07.

12. Поднебенна С. К., Бурлака В. В., Гулаков С. В., Кисляк В. Г. Модернізація розривної машини 2167Р-50 для дослідження міцності зварних з'єднань // Вісник Приазовського державного технічного університету. Технічні науки. – 2018. – № 36. – С. 113–119. – DOI: https://doi.org/10.31498/2225-6733.36.2018.142532.

13. Алексенко В. Л., Юренін К. Ю., Татарінцева Ю. Г., Фостик П. П., Васильченко Г. Ю., Знамеровська Н. П., Онишко Д. М. Схемотехнічні рішення при реновації випробувального обладнання // Науковий вісник Херсонської державної морської академії. – 2024. – № 1(28). – С. 93–103. – DOI: https://doi.org/10.33815/2313-4763.2024.1.28.093-103.

14. Protsenko, V., Malashchenko, V., Babii, M., Nastasenko, V., Protasov, R., Brumerčík, F., & Macko, M. (2025). Redundant constraints in crane disc brake mechanism: Effect and disposal perspectives. *Communications – Scientific Letters of the University of Žilina, 29*. DOI: https://doi.org/10.26552/com.C.2025.029

15. Meneghini, L., Noal Artmann, V., Simoni, R., & Simas, H. (2021). Mobility analysis and self-alignment of a novel asymmetric 3T parallel manipulator. In M. Pucheta, A. Cardona, S. Preidikman, & R. Hecker (Eds.), *Multibody Mechatronic Systems. MuSMe 2021. Mechanisms and Machine Science* (Vol. 94, pp. 133–144). Springer. DOI: https://doi.org/10.1007/978-3-030-60372-4_11